

Compressibility and consolidation properties of Santos soft clay near Barnabé Island

Vitor Nascimento Aguiar^{1#} , Maurício do Espírito Santo Andrade² ,

Ian Schumann Marques Martins³ , Jean Pierre Paul Rémy⁴ ,

Paulo Eduardo Lima de Santa Maria⁵ 

Article

Keywords

Santos soft clay
Geotechnical characterization
One-dimensional consolidation test
Sample quality
Remolding effects
Strain-rate effects

Abstract

A geotechnical study based on characterization tests and seventy incremental loading one-dimensional consolidation tests was carried out on high-quality undisturbed samples taken from Santos Harbor Channel subsoil near to Barnabé Island, where a pilot embankment was built. The characterization profiles revealed a stratigraphy following the pattern described by Massad (2009), with a 9 m-thick fluvial-lagoon-bay sediments (SFL) clay layer. The consolidation tests were performed following two loading criteria. In criterion A (series one tests), a new loading was applied whenever the strain rate ($\dot{\epsilon}$) reached 10^{-6} s^{-1} , the highest integer power of 10 after the “end of primary” consolidation for double drained 2 cm-thick specimens. In criterion B (series two tests), the standard procedure of 24 hour-long stages was adopted. Criterion A reduced the total duration of the consolidation tests from ten to about three days. The preconsolidation (yield) stress (σ'_p) and the compressibility parameters C_c and C_r obtained from “ e versus σ'_v (log)” compression curves of all tests are provided. Series two tests showed that the 24-hour “ e versus σ'_v (log)” compression curves are translated to the left of the $\dot{\epsilon} = 10^{-6} \text{ s}^{-1}$ “ e versus σ'_v (log)” compression curves, keeping C_r and C_c average values unchanged, but decreasing σ'_p by about 8%. The SFL clay $C_c/(1+e_0)$ values obtained herein are higher than those presented by Massad (2009) due to the higher-quality samples tested in this study. It is shown that it is feasible to carry out a high-quality laboratory test program for design purposes following current standards.

1. Introduction

The city of Santos is in the coast of São Paulo State, 80 km far from the city of São Paulo. The Santos lowlands consist of thick layers of soft clayey soils, which imply important civil engineering problems due to their high compressibility and low shear strength. In the last few decades, several geotechnical studies have been carried out on the Santos soft clays (Massad, 2009).

According to Suguio & Martin (1994), the fluctuations in sea level during the Quaternary was the main mechanism that formed the marine sediments of the São Paulo State coastal plains. Two transgressive episodes would have been responsible for different types of sediments. The first, called Cananea

Transgression, occurred in the Pleistocene between 100,000 and 120,000 years ago, when the sea level was probably 8 ± 2 m above the present sea level. The second episode, called Santos Transgression, occurred in the Holocene (last 11,000 years), when the sea level reached its maximum between 2.3 m and 5.0 m above the present level 5100 years ago.

Massad (1985) proposed a genetic classification for the Santos lowlands clays, grouping them into three main units: Mangrove clays, SFL clays and Transitional clays. Massad (2009, Table 5.1) described the Mangrove clays as “modern” deposits that show preconsolidation (yield) stress (σ'_p) ≤ 30 kPa, void ratio (e) > 4 and SPT blow count (N) = 0. SFL clays (fluvial-lagoon-bay sediments) were deposited during the Santos Transgression about 5000-7000 years

[#]Corresponding author. E-mail address: vitornaguair@hotmail.com

¹Pontifícia Universidade Católica do Rio de Janeiro, Department of Civil and Environmental Engineering, Rio de Janeiro, RJ, Brasil.

²Universidade Tecnológica Federal do Paraná, Department of Civil Engineering, Toledo, PR, Brasil.

³Universidade Federal do Rio de Janeiro, Graduate School and Research in Engineering, Department of Civil Engineering, Rio de Janeiro, RJ, Brasil.

⁴Mecasolo Engenharia e Consultoria Eireli, Nova Friburgo, RJ, Brasil.

⁵SM Engenheiros Consultores Ltda, Rio de Janeiro, RJ, Brasil.

Submitted on September 5, 2021; Final Acceptance on November 10, 2021; Discussion open until February 28, 2022.

<https://doi.org/10.28927/SR.2021.074821>



This is an Open Access article distributed under the terms of the Creative Commons Attribution License, which permits unrestricted use, distribution, and reproduction in any medium, provided the original work is properly cited.

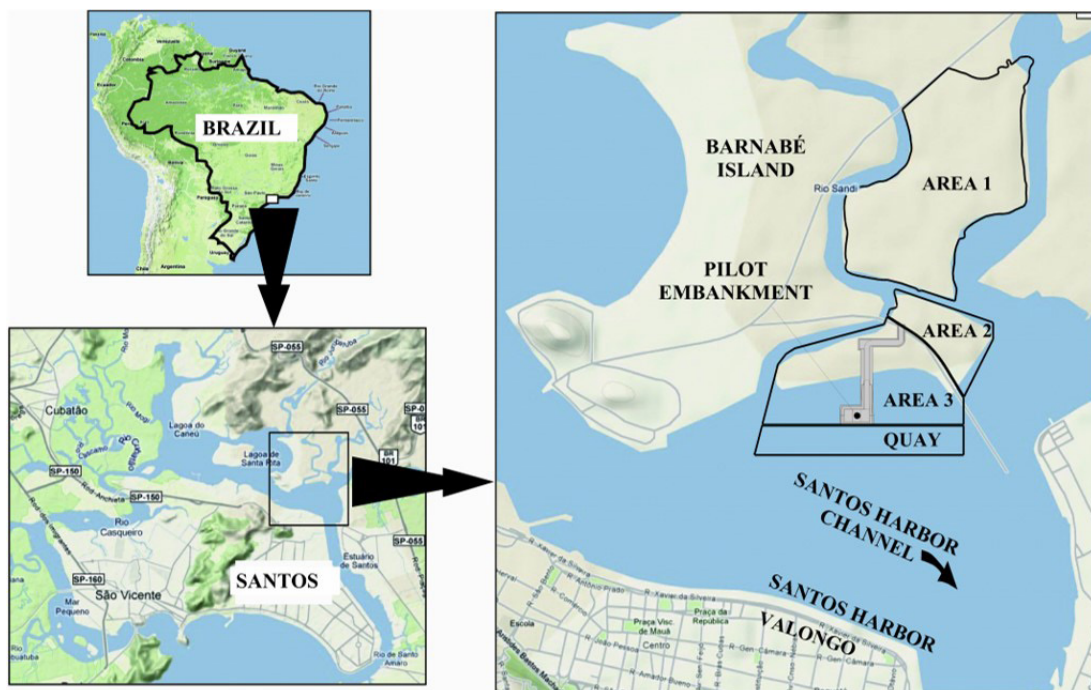


Figure 1. Pilot embankment site (adapted from Rémy et al., 2011).

ago, with $30 \text{ kPa} \leq \sigma'_p \leq 200 \text{ kPa}$, $2 \leq e \leq 4$ and $0 \leq N \leq 4$. Transitional clays, deposited in a mixed continental-marine environment during the Cananea Transgression, have $200 \text{ kPa} \leq \sigma'_p \leq 700 \text{ kPa}$, $e < 2$ and $5 \leq N \leq 25$. Massad (2009) provided a complete characterization, physical indexes and compressibility, consolidation and shear strength parameters of the three genetic units.

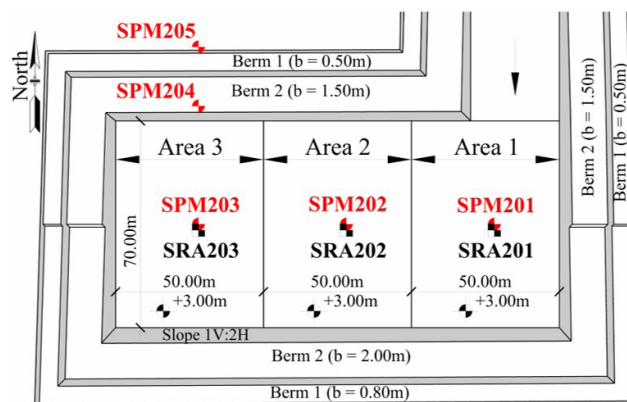
The Santos harbor is the largest and most important port complex in Latin America. There are currently several expansion projects alongside the Santos harbor channel. A multipurpose terminal covering an area of $800,000 \text{ m}^2$ was built on Barnabé Island, on the left bank of the Santos harbor channel (Figure 1). An instrumented pilot embankment was built in 2007 to provide field compressibility, consolidation and shear strength data of the soft clay foundation deposit (Rémy et al. 2011). A comprehensive laboratory test program on high-quality samples as well as *in situ* geotechnical investigation were also carried out.

The purpose of this paper is to present the characterization test results and the compressibility and consolidation parameters obtained from one-dimensional consolidation tests of the subsoil samples taken in the pilot embankment area before its construction.

2. Materials and methods

2.1 Sampling, transportation and storage

Figure 2 shows the boreholes location for standard penetration tests (SPM) and for taking undisturbed samples (SRA) in the pilot embankment area. The undisturbed samples



Legend: ■ SPM - Borehole for standard penetration tests
■ SRA - Borehole for taking undisturbed samples

Figure 2. Boreholes location in the pilot embankment area (adapted from Rémy et al., 2011).

taken from borehole SRA203 were sent to the Soil Rheology Laboratory of the Federal University of Rio de Janeiro, where they were tested. The samples taken from boreholes SRA201 and SRA202 were tested in another laboratory and are not presented herein.

To take good-quality samples, ABNT (1997) and “Technical specification for taking undisturbed samples” (Aguiar, 2008) were followed. 10 cm-inner diameter and 70 cm-long thin-wall fixed piston samplers were used. The samples were taken by a team trained by two of the authors when taking the first samples. Figure 3 shows the position of the twelve undisturbed samples taken from borehole SRA203 along the borehole SPM203 profile.

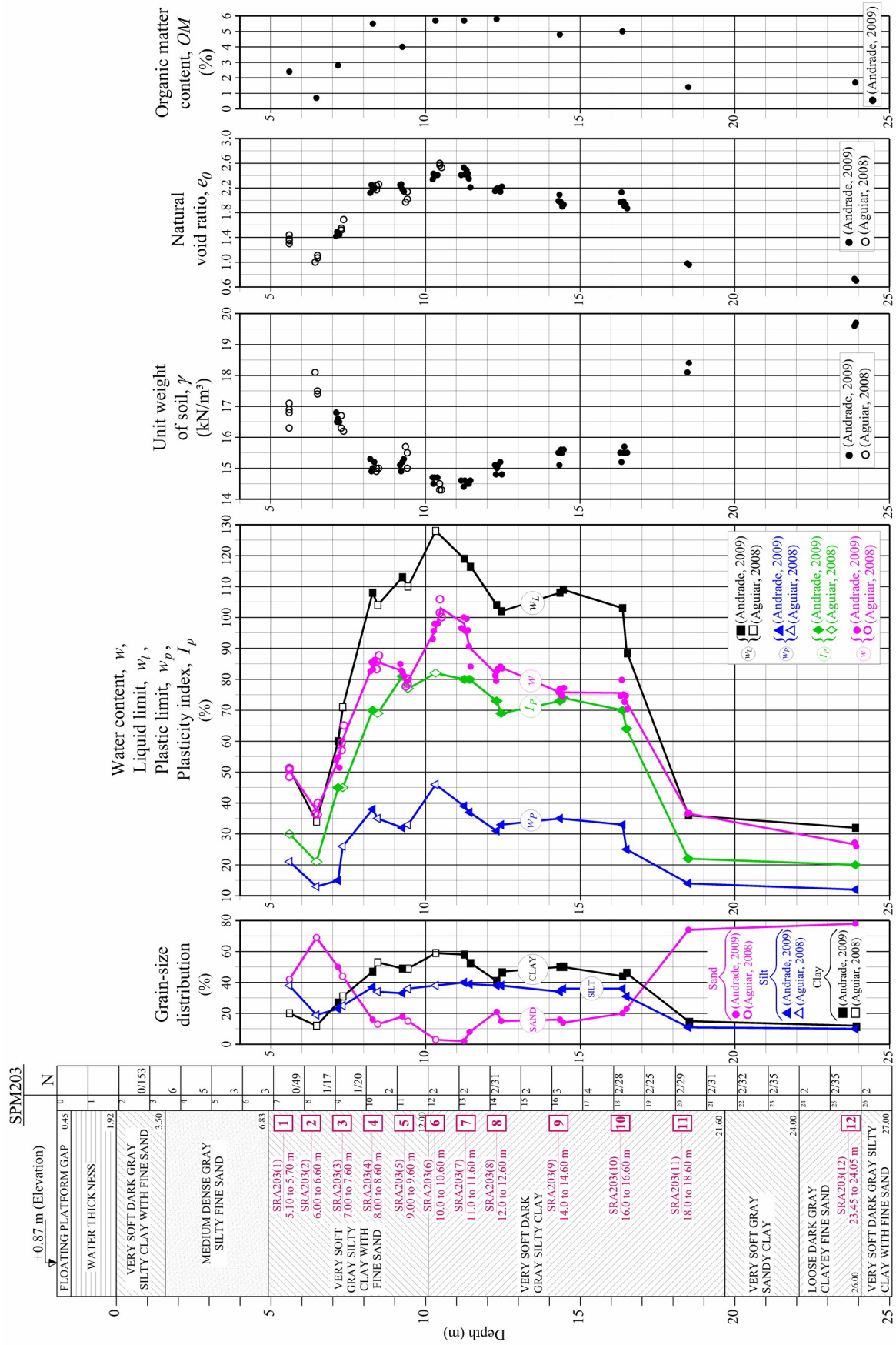


Figure 3. Subsoil profile based on borehole SPM203 and characterization test results carried out on SRA203 samples.

The borehole SPM203 showed a first layer of very soft clay 1.60 m thick with $N = 0$. According to the Massad (2009) genetic classification, this layer is a Mangrove clay. It must be recognized that $N = 0$ terminology comprises a wide range of soft clay consistencies, that goes from P/30, meaning a 30 cm penetration of the SPT sampler under the hammer's weight, to 0/XXX, where XXX means the penetration in centimeters of the SPT sampler under the rod set weight only. For instance, in Figure 3, at 1.0 m depth the symbol 0/153 means that the SPT sampler penetrated 153 cm under the rod set weight. Such consistency range is usually found in Santos Mangrove clay layers. Underlying this clay layer, there is a 3.30 m-thick sand layer with N between 3 and 6. The first undisturbed sample was taken 10 cm below the bottom of this sand layer (Figure 3).

The sample ends were covered with PVC film and aluminum foil and sealed with paraffin wax. The sampler tip was protected against bumps with a 10 cm-high PVC rigid ring. The samples were shipped in vertical position into wood containers with the tip downwards (ASTM, 2007). After sampling,

the samplers were placed into the wood containers, stored in a room protected from the sun, where people circulation was not allowed. After taking the last sample, the containers were sent to the laboratory and stored in a humid room.

2.2 Geotechnical characterization

Table 1 shows grain-size distribution (ABNT, 1995), liquid limit (w_L), plastic limit (w_p), plasticity index (I_p), specific gravity (G_s) and organic matter content (OM) obtained for the indicated segments of each SRA203 sample (second column of Table 1). Water content (w), unit weight of soil (γ), natural void ratio (e_0) and degree of saturation (S_r) are the average values obtained from the undisturbed consolidation test specimens belonging to each sample segment.

Figure 3 shows the subsoil profile according to tactile-visual examination of the SPT samples from borehole SPM203 only. Figure 3 also shows the laboratory characterization test results carried out on SRA203 samples and w , γ and e_0 values are plotted for all undisturbed consolidation test specimens.

Table 1. Characterization test results of samples SRA203(1) to SRA203(12).

Sample	Depth ^(a) (m)	w (%)	G_s	S_r (%)	e_0	γ (kN/m ³)	Atterberg Limits (%)			Grain-size distribution (%)			OM (%)
							w_L	w_p	I_p	sand	silt	clay	
SRA203(1)	5.55 - 5.65	50.5	2.64	98	1.37	16.8	51	21	30	42	38	20	2.4
SRA203(2)	6.40 - 6.55	37.6	2.65	94	1.06	17.7	34	13	21	69	19	12	0.7
SRA203(3)	7.10 - 7.25	53.7	2.63	98	1.46	16.6	60	15	45	50	23	27	2.8
	7.25 - 7.40	60.6	2.64	99	1.59	16.4	71	26	45	44	25	31	-
SRA203(4)	8.20 - 8.38	84.4	2.60	100	2.18	15.1	108	38	70	16	37	47	5.5
	8.38 - 8.53	85.6	2.60	100	2.22	15.0	104	35	69	13	34	53	-
SRA203(5)	9.17 - 9.34	82.7	2.65	99	2.21	15.1	113	32	81	18	33	49	4.0
	9.34 - 9.45	78.8	2.62	99	2.04	15.4	110	33	77	15	36	49	-
SRA203(6)	10.22 - 10.43	96.1	-	100	2.40	14.7	-	-	-	-	-	-	5.7
	10.43 - 10.55	103	2.53	100	2.57	14.4	128	46	82	3	38	59	-
SRA203(7)	11.14 - 11.36	98.0	-	100	2.46	14.6	119	39	80	2	40	58	5.7
	11.36 - 11.49	90.2	2.55	98	2.33	14.5	117	37	80	8	39	53	-
SRA203(8)	12.24 - 12.36	81.7	2.59	99	2.18	15.0	104	31	73	21	38	41	5.8
	12.40 - 12.50	83.8	2.62	99	2.18	15.0	102	33	69	15	38	47	-
SRA203(9)	14.29 - 14.40	75.8	2.63	99	2.01	15.4	108	35	73	16	34	50	4.8
	14.40 - 14.50	75.8	2.58	100	1.92	15.6	109	35	74	14	36	50	-
SRA203(10)	16.29 - 16.45	75.6	2.64	100	2.00	15.5	103	33	70	20	36	44	5.0
	16.45 - 16.55	72.6	2.60	99	1.90	15.5	89	25	64	23	31	46	-
SRA203(11)	18.45 - 18.55	36.6	2.63	99	0.97	18.3	36	14	22	74	11	15	1.4
SRA203(12)	23.85 - 23.95	26.6	2.66	99	0.72	19.7	32	12	20	78	10	12	1.7

^(a)The depths indicated are not the depths at the top and bottom of the undisturbed samples as shown in Figure 3, but rather the depths of segments of the samples where the undisturbed consolidation test specimens were trimmed.

Samples SRA203(1), SRA203(2) and SRA203(3) test results revealed that the subsoil profile corresponding to their depths should be better described as “silty clayey sand”. According to sample SRA203(11) test results, the subsoil profile at its depth should be better described as “clayey sand”.

2.3 One-dimensional consolidation test procedure

Incremental loading one-dimensional consolidation tests were carried out on the twelve samples from borehole SRA203.

Long-term loading stages were run in selected tests to investigate secondary consolidation and stress relaxation. However, these results are outside the scope of this paper.

2 cm-high and 7 cm-diameter specimens were trimmed following Ladd and DeGroot (2003) recommendations and additional cares described by Aguiar (2008) and Andrade (2009).

Specimens are identified by the acronym CPMX, where CP means specimen, M is the sample number and X the letter that denotes the order position of the specimen in sample M, for instance: CP6E is the fifth (letter E) specimen trimmed in sample SRA203(6). Tables A1 and A2 (see Appendix) indicate the depth interval from which each specimen was trimmed.

All tests were carried out on Bishop-type consolidation frames, with settlements being measured by 0.01 mm/division dial gages, under temperature of 20 ± 1 °C. Temperature variations were daily monitored by a *maximum* and *minimum* thermometer.

Each consolidation test was performed using one out of two loading criteria: criterion A, based on the specimen vertical strain rate ($\dot{\epsilon}$), and criterion B, based on stage duration.

In criterion A, a new loading stage was applied whenever the vertical strain rate ($\dot{\epsilon}$) reached 10^{-6} s^{-1} , calculated as:

$$\dot{\epsilon} = \frac{1}{\Delta t} \left(\frac{\Delta H}{H} \right) \quad (1)$$

where:

H : specimen height corresponding to reading of order i ;

ΔH : settlement difference ($H_i - H_{i+1}$);

Δt : time elapsed between readings of orders i and $i + 1$.

For samples SRA203(4) to SRA203(10), it was observed that $\dot{\epsilon} = 10^{-6} \text{ s}^{-1}$ corresponded to the higher integer power of 10 after the “end of primary” consolidation, calculated by both Taylor (1942) (\sqrt{t}) and Casagrande ($\log(t)$) methods of coefficient of consolidation (c_v) determination for specimens whose drainage path is about 1 cm.

A first series of consolidation tests (“series one”) was performed on all twelve samples using criterion A. The following specimens were tested:

- four undisturbed specimens from sample SRA203(1),
- three undisturbed specimens and one remolded specimen from each out of samples SRA203(2) to SRA203(7),
- two undisturbed specimens from each out of samples SRA203(8) to SRA203(12), totalizing thirty eight

tests, being thirty two on undisturbed specimens and six on remolded specimens.

Remolding was done prior to specimen trimming, by smashing an amount of sample inside a plastic bag. Consolidation tests on remolded specimens were carried out to check the quality of the undisturbed specimens by comparing their results.

All tests in series one underwent the following loading sequence up to 100 kPa: 3.13, 6.25, 12.5, 25, 50 and 100 kPa. From 100 kPa on, the loading and unloading sequences followed different patterns, as shown in Table 2. In some tests, a loading stage was selected to monitor secondary consolidation under a chosen overconsolidation ratio (OCR). In other tests, stress relaxation was observed by preventing specimen settlements. These stages were analyzed by Aguiar (2008) and Andrade (2009).

In tests with specimens CP7A, CP7B, CP7C and CP7D, influence of temperature was investigated in loading stages beyond 300 kPa. As σ'_p values of these specimens are not greater than 160 kPa and the compression index (C_c) values were determined in the virgin compression curves immediately after σ'_p , the C_c values obtained were not affected by the loading stages in which temperature effects were investigated.

A second series of consolidation tests (“series two”) was carried out using criterion B, in which four undisturbed specimens were tested from each out of samples SRA203(3) to SRA203(10), totalizing thirty two tests.

In criterion B, the loading stages lasted 24 hours and the loading sequence was 3.13, 6.25, 12.5, 25, 50, 100, 150, 200, 300, 500 and 800 kPa, followed by unloading to 400 and 200 kPa, except for specimens CP8C, CP8D, CP8E and CP8F, which were unloaded to different stresses in order to investigate secondary consolidation under different OCR values, as shown in Table 3. These unloading stages were analyzed by Andrade (2009).

Stress increment ratio ($\Delta\sigma/\sigma$) < 1 in the loading sequence of series two was intended to determine σ'_p with more accuracy and to define more clearly the compression curve.

Hence, seventy consolidation tests were run in the two test series, being sixty four on undisturbed specimens and six on remolded ones.

3. Test results

Vertical strain (ϵ) versus vertical effective stress (σ'_v) (\log) and void ratio (e) versus σ'_v (\log) compression curves of series one specimens were plotted with ϵ and e of each loading stage corresponding to:

- a) “end of primary” consolidation calculated by Taylor’s (1942) method and
- b) vertical strain rate ($\dot{\epsilon}$) of 10^{-6} s^{-1} .

ϵ versus σ'_v (\log) and e versus σ'_v (\log) compression curves of series two specimens were plotted with ϵ and e of each loading stage corresponding to:

- a) “end of primary” consolidation calculated by Taylor’s (1942) method,

Table 2. Loading and unloading sequences from 100 kPa on of series one specimens.

Specimen	Loading and unloading sequences (kPa)
CP1A	100/200 (sec. cons. for 42 days, $OCR=1.00$)/400/350/200/100
CP1B	100 - 200 (stress relax. for 42 days) - 400 - 350 - 200 - 100
CP1C	100 - 250 - 200 (sec. cons. for 42 days, $OCR=1.25$) - 250 - 400 - 350 - 200 - 100
CP1D	100 - 300 - 200 (sec. cons. for 42 days, $OCR=1.50$) - 300 - 400 - 350 - 200 - 100
CP2A	100 - 200 (sec. cons. for 19 days, $OCR=1.00$) - 400 - 800 - 400 - 200
CP2B	100 - 200 (stress relax. for 19 days) - 400 - 800 - 400 - 200
CP2C	100 - 250 - 200 (sec. cons. for 19 days, $OCR=1.25$) - 250 - 400 - 800 - 400 - 200
CP2D ^(a)	100 - 200 - 50 (sec. cons. for 19 days, $OCR=4.00$) - 100 - 200 - 400 - 800 - 400 - 200
CP3A	100 - 200 (sec. cons. for 17 days, $OCR=1.00$) - 400 - 800 - 400 - 200
CP3B	100 - 200 (stress relax. for 17 days) - 400 - 800 - 400 - 200
CP3C	100 - 250 - 200 (sec. cons. for 17 days, $OCR=1.25$) - 250 - 400 - 800 - 400 - 200
CP3D ^(a)	100 - 200 - 50 (sec. cons. for 17 days, $OCR=4.00$) - 100 - 200 - 400 - 800 - 400 - 200
CP4A	100 - 200 (sec. cons. for 19 days, $OCR=1.00$) - 400 - 800 - 400 - 200
CP4B	100 - 200 (stress relax. for 19 days) - 400 - 800 - 400 - 200
CP4C	100 - 300 - 200 (sec. cons. for 19 days, $OCR=1.50$) - 300 - 400 - 800 - 400 - 200
CP4D ^(a)	100 - 200 - 100 - 50 (sec. cons. for 19 days, $OCR=4.00$) - 100 - 200 - 400 - 800 - 400 - 200
CP5A	100 - 150 - 200 (sec. cons. for 47 days, $OCR=1.00$) - 300 - 400 - 800 - 400 - 200
CP5B	100 - 150 - 200 - 300 (stress relax. for 47 days) - 400 - 800 - 400 - 200
CP5C	100 - 150 - 200 - 300 - 200 (sec. cons. for 47 days, $OCR=1.50$) - 300 - 400 - 800 - 400 - 200
CP5D ^(a)	100 - 200 - 100 - 50 (sec. cons. for 47 days, $OCR=4.00$) - 100 - 200 - 400 - 800 - 400 - 200
CP6A	100 - 150 - 200 - 400 (sec. cons. for 42 days, $OCR=1.00$) - 800 - 400 - 200
CP6B	100 - 150 - 200 - 400 - 720 - 400 (sec. cons. for 42 days, $OCR=1.80$) - 720 - 800 - 400 - 200
CP6C	100 - 150 - 200 - 400 - 640 - 400 (sec. cons. for 42 days, $OCR=1.60$) - 640 - 800 - 400 - 200
CP6D ^(a)	100 - 200 - 100 - 50 (sec. cons. for 42 days, $OCR=4.00$) - 100 - 200 - 400 - 800 - 400 - 200
CP7A	100 - 150 - 200 - 400 - 300 (sec. cons. for 60 days, $OCR=1.33$, $20^{\circ}\text{C} \rightarrow 35^{\circ}\text{C}$) - 400 (sec. cons. for 66 days, $OCR=1.00$, 35°C) - 650 ($35^{\circ}\text{C} \rightarrow 20^{\circ}\text{C}$) - 1000 - 500 (sec. cons. for 59 days, $OCR=2.00$) - 250
CP7B	100 - 150 - 200 - 450 (stress relax. for 60 days, $20^{\circ}\text{C} \rightarrow 35^{\circ}\text{C}$; sec. cons. for 23 days, $OCR = 1,00$, 35°C ; stress relax. for 44 days, 35°C) - 650 ($35^{\circ}\text{C} \rightarrow 20^{\circ}\text{C}$) - 1000 - 500 (sec. cons. for 59 days, $OCR=2.00$) - 250
CP7C	100 - 150 - 200 - 500 - 300 (sec. cons. for 60 days, $20^{\circ}\text{C} \rightarrow 35^{\circ}\text{C}$) - 400 (sec. cons. for 66 days, 35°C) - 650 ($35^{\circ}\text{C} \rightarrow 20^{\circ}\text{C}$) - 1000 - 500 - 250 (sec. cons. for 57 days, $OCR=4.00$)
CP7D ^(a)	100 - 200 - 400 - 800 - 400 - 200 (sec. cons. for 186 days, $OCR=4.00$, $20^{\circ}\text{C} \rightarrow 35^{\circ}\text{C} \rightarrow 20^{\circ}\text{C}$)
CP8A	100 - 150 - 200 - 400 - 800 - 400 - 200
CP8B	100 - 150 - 200 - 400 - 800 - 400 - 200
CP9A	100 - 150 - 200 - 300 - 500 - 800 - 400 - 200
CP9B	100 - 150 - 200 - 300 - 500 - 800 - 400 - 200
CP10A	100 - 200 - 300 - 500 - 800 - 400 - 200
CP10B	100 - 200 - 300 - 500 - 800 - 400 - 200
CP11A	100 - 200 - 300 - 500 - 800 - 400 - 200
CP11B	100 - 200 - 300 - 500 - 800 - 400 - 200
CP12A	100 - 200 - 300 - 400 - 600 - 800 - 400 - 200
CP12B	100 - 200 - 300 - 400 - 600 - 800 - 400 - 200

^(a)specimen remolded in the laboratory; sec.cons.: secondary consolidation; stress relax.: stress relaxation (settlement prevented).

Table 3. Unloading sequence from 800 kPa of series two SRA203(8) specimens.

Specimen	Unloading sequence (kPa)
CP8C	800 - 350 (secondary consolidation for 20 days, $OCR=2.29$) - 200
CP8D	800 - 400 (secondary consolidation for 20 days, $OCR=2.00$) - 200
CP8E	800 - 300 (secondary consolidation. for 20 days, $OCR=2.67$) - 200
CP8F	800 - 500 (secondary consolidation for 20 days, $OCR=1.60$) - 200

- b) vertical strain rate ($\dot{\epsilon}$) of 10^{-6} s^{-1} and
- c) end of 24 hours.

Compression curves plotted in terms of void ratio (e) according to the criteria mentioned above were compared. Figure 4 shows an example of such comparison for specimen CP5E, from series two. The comparisons of all the other

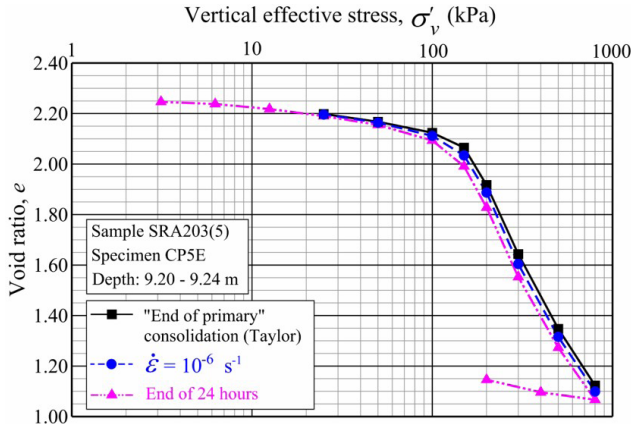


Figure 4. e versus $\sigma'_v(\log)$ curves of specimen CP5E.

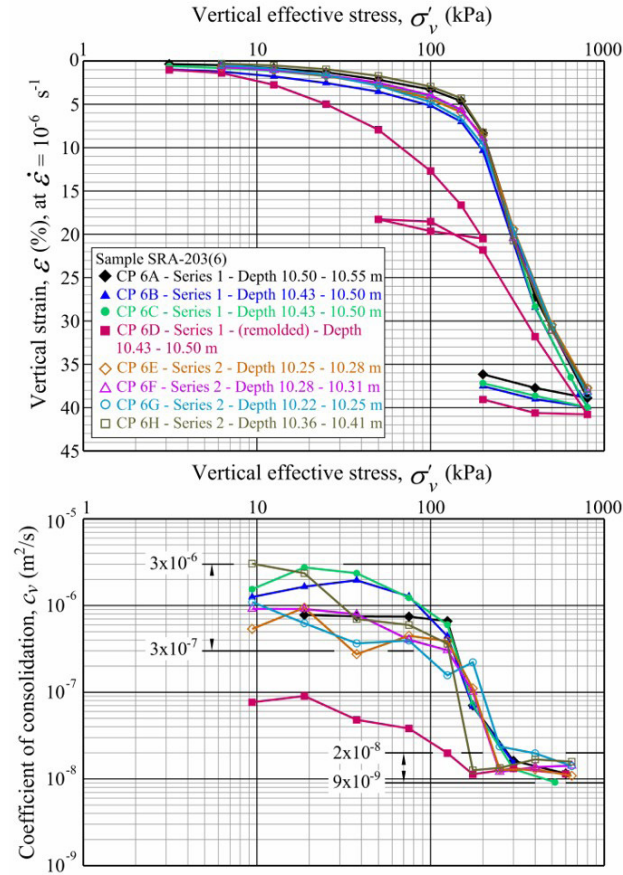


Figure 5. ϵ versus $\sigma'_v(\log)$ curves corresponding to $\dot{\epsilon} = 10^{-6} \text{ s}^{-1}$ and $c_v(\log)$ versus average $\sigma'_v(\log)$ curves of all SRA203(6) specimens (adapted from Rémy et al., 2011).

specimens were presented by Aguiar (2008) and Andrade (2009). As observed in all tests, the 24-hour compression curve lies below the $\dot{\epsilon} = 10^{-6} \text{ s}^{-1}$ compression curve, which, in its turn, lies below the “end of primary” compression curve.

From 12.5 kPa on, c_v values were determined by Taylor’s (1942) method and plotted against the average σ'_v values of the respective loading stages. ϵ versus $\sigma'_v(\log)$ and e versus $\sigma'_v(\log)$ compression curves corresponding to “end of primary”, $\dot{\epsilon} = 10^{-6} \text{ s}^{-1}$ and 24 hours, together with the $c_v(\log)$ versus average $\sigma'_v(\log)$ curves, of all seventy specimens were presented by Aguiar (2008) and Andrade (2009). Figure 5 shows the ϵ versus $\sigma'_v(\log)$ curves corresponding to $\dot{\epsilon} = 10^{-6} \text{ s}^{-1}$ and the $c_v(\log)$ versus average $\sigma'_v(\log)$ curves of all SRA203(6) specimens. Specimen CP6D was remolded. Figure 6 shows the ϵ versus $\sigma'_v(\log)$ curves corresponding to 24 hours and the $c_v(\log)$ versus average $\sigma'_v(\log)$ curves of series two SRA203(8) specimens. The excellent repeatability of the results obtained for the SRA203(6) and SRA203(8) specimens (Figures 5 and 6) was also observed in all SRA203(4) to SRA203(10) specimens, which belong to the SFL clay layer, as discussed further.

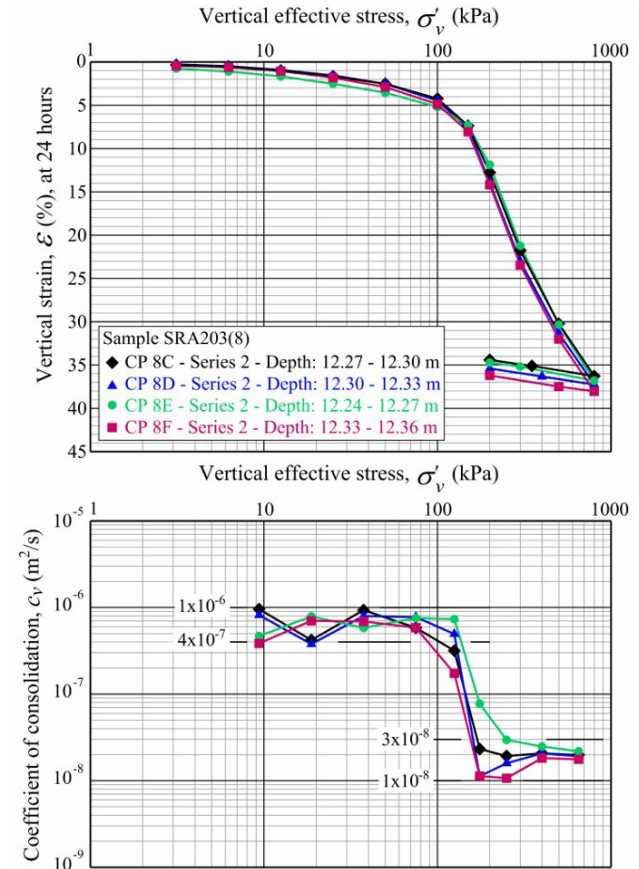


Figure 6. ϵ versus $\sigma'_v(\log)$ curves corresponding to 24 hours and $c_v(\log)$ versus average $\sigma'_v(\log)$ curves of series two SRA203(8) specimens.

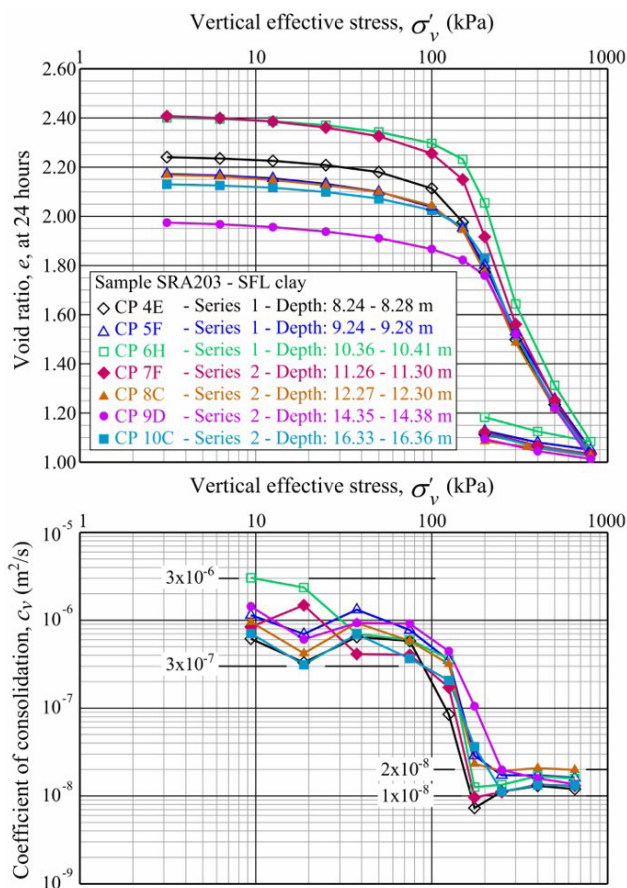


Figure 7. e versus $\sigma'_v(\log)$ typical curves corresponding to 24 hours and their respective $c_v(\log)$ versus average $\sigma'_v(\log)$ curves from samples SRA203(4) to SRA203(10).

Figure 7 gathers typical e versus $\sigma'_v(\log)$ curves corresponding to 24 hours and their respective $c_v(\log)$ versus average $\sigma'_v(\log)$ curves from one undisturbed specimen of each sample from SRA203(4) to SRA203(10). Compression curves for samples SRA203(1), SRA203(2), SRA203(3), SRA203(11) and SRA203(12) are not included since they are sand. Figure 7 shows that, for practical purposes, samples SRA203(4) to SRA203(10) can be assumed to belong to a single “homogeneous” clay layer.

The preconsolidation (yield) stress (σ'_p), compression index (C_c) and recompression index (C_r) were obtained for all specimens (series one and two) from e versus $\sigma'_v(\log)$ curves corresponding to $\dot{\epsilon} = 10^{-6} \text{ s}^{-1}$ as shown in Table A1 (see Appendix A), which also shows $C_c/(1+e_0)$ and C_r/C_c values. The same parameters, including the swelling index (C_s), were also obtained for series two specimens from e versus $\sigma'_v(\log)$ curves corresponding to 24 hours as shown in Table A2 (see Appendix A), which also shows $C_c/(1+e_0)$ and C_r/C_c values. All C_s values correspond to an $OCR = 4$. The σ'_p values were obtained according to Silva (1970) method. The C_r , C_c and C_s values were determined as shown in Figure 8. σ'_{v0} is the effective overburden stress.

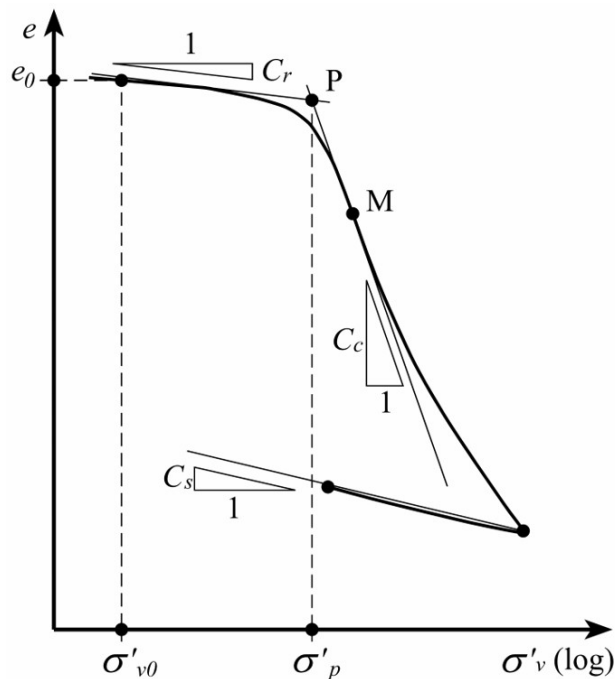


Figure 8. Procedure for determining C_r , C_c e C_s values.

Figure 9 shows the profiles of σ'_p , $C_c/(1+e_0)$ and C_r/C_c obtained from e versus $\sigma'_v(\log)$ curves corresponding to $\dot{\epsilon} = 10^{-6} \text{ s}^{-1}$ of all specimens (series one and two - Table A1), and from e versus $\sigma'_v(\log)$ curves corresponding to 24 hours of all series two specimens (Table A2).

4. Discussion

4.1 Stratigraphy and characterization

Figure 10 shows the stratigraphy of the subsoil based on borehole SPM203 SPT samples, characterization tests and physical indexes of the undisturbed samples as well as on tactile-visual examination when trimming the consolidation test specimens.

Since no undisturbed samples were obtained from the mangrove clay layer, a unit weight of 13.0 kN/m^3 was assigned to it based on Massad (2009, pp. 106). The existence of this layer was confirmed *in situ* via SPT samples examination. As no undisturbed samples were obtained from the top sand layer, a unit weight of 20.0 kN/m^3 was assigned to it since this layer is sandier than SRA203(12) sample, which unit weight is 19.7 kN/m^3 (Table 1).

Between the top sand layer and the SFL clay layer, there is a transition layer composed by three sandy sublayers identified based on samples SRA203(1), SRA203(2) and SRA203(3) characterization tests and physical indexes.

Samples SRA203(4) to SRA203(10) characterization tests and physical indexes revealed that they belong to a single SFL clay layer according to the Massad (2009) genetic

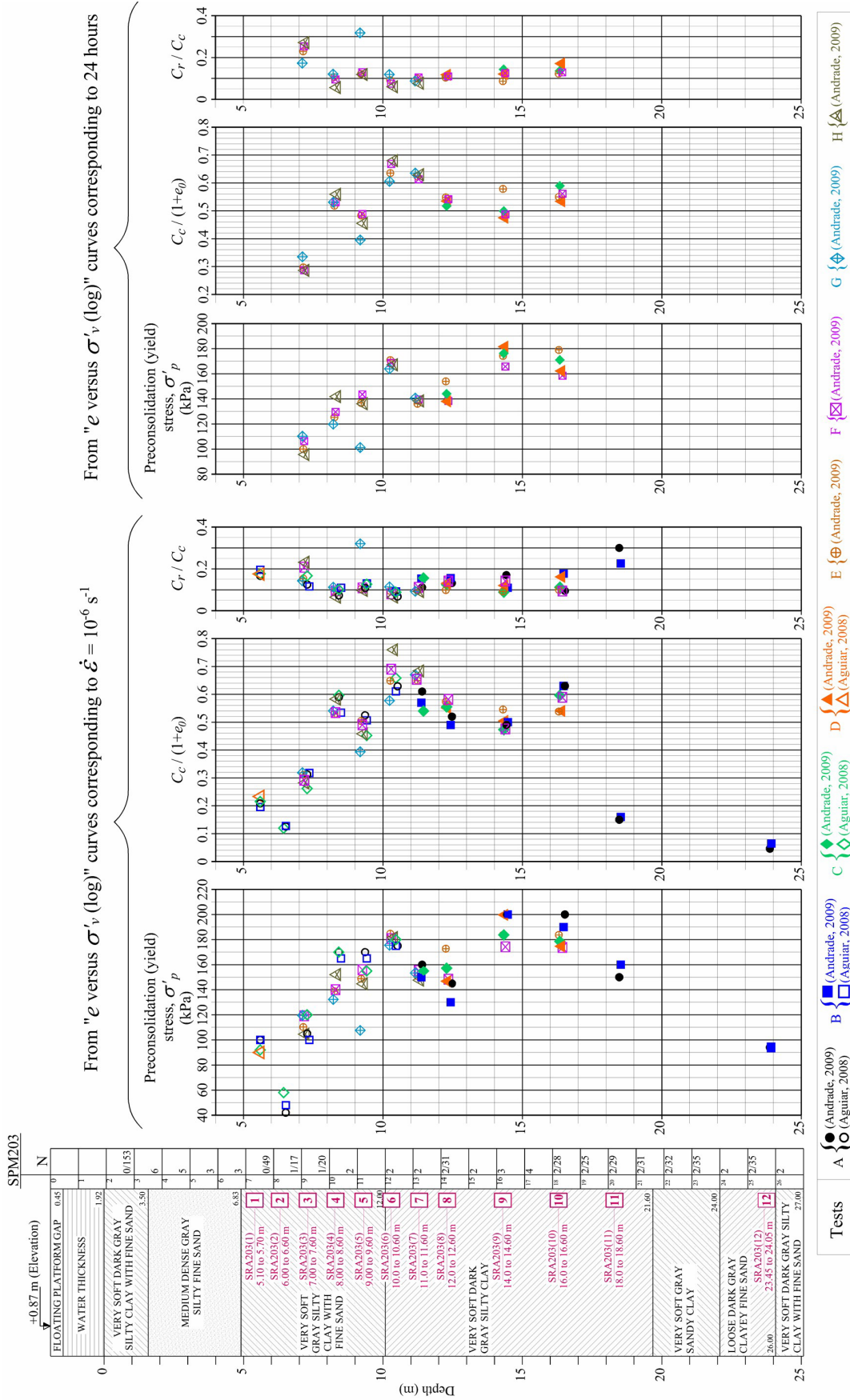


Figure 9. Profiles of σ'_p , $C_c/(1+e_p)$ and C_r/C_c from "e versus σ'_v (log)" curves corresponding to $\dot{\epsilon} = 10^{-6} \text{ s}^{-1}$ and to 24 hours.

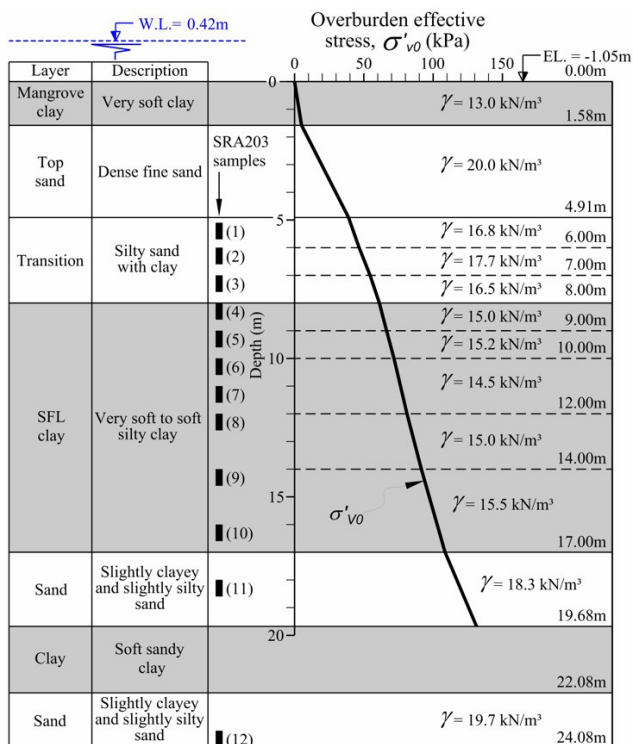


Figure 10. Geotechnical profile of the subsoil.

classification. It is worth noting the increase of water content and plasticity from sample SRA203(3) to SRA203(4), as well as the decrease of water content and plasticity from sample SRA203(10) to SRA203(11). Samples SRA203(6) and SRA203(7) have water content, void ratio, liquid limit and clay content higher than the others. Presence of kaolinite, smectite and illite was identified along the SFL clay layer by X-ray diffraction.

Samples SRA203(11) and SRA203(12) characterization tests and physical indexes showed that they belong to sand layers below the SFL clay layer.

The unit weights shown in Figure 10 are the average values from undisturbed consolidation test specimens of each sample and the effective overburden stress (σ'_{v0}) profile was estimated with these unit weights.

4.2 Sample quality and remolding effects on one-dimensional compression curves

The comparisons between compression curves of remolded and undisturbed specimens (Figure 5) highlighted the following remolding effects (Ladd, 1973):

- 1) Decreases the void ratio (or increases the strain) at any given σ'_v value;
- 2) Makes it difficult to define the point of minimum radius, thus obscuring σ'_p ;
- 3) Lowers the estimated value of σ'_p ;

- 4) Increases the compressibility in the recompression region;
- 5) Decreases the compressibility in the virgin compression region.

Coutinho (1976) and Martins (1983) have also observed that remolding turns the concave shape of the virgin compression curve into a straight line. As σ'_v increases, structure of undisturbed specimens is destroyed, making their behavior approach to that of the remolded specimen. Thus, as σ'_v increases, the compression curves of all specimens tend to merge into a single curve (Figure 5).

Another remarkable feature of high-quality specimens is the abrupt fall of the c_v versus σ'_v (log) curves when σ'_v straddles σ'_p . Such fall may be of two orders of magnitude (Figures 5, 6 and 7). This is not observed in the c_v versus σ'_v (log) curve of the remolded specimen (Figure 5). The smaller c_v values in the recompression region of the remolded specimen are due to the compressibility increase in the recompression region caused by remolding.

Although not shown herein, no difference at all was observed between the compression curve of the remolded specimen and those of the “undisturbed” specimens trimmed on sample SRA203(2), which is 69% sand (Aguiar, 2008).

Regarding footnote (b) in Table A1, C_r values could not be obtained according to Figure 8 since remolding pushed σ'_p to a value lower than σ'_{v0} .

Table 4 shows the quality classification of series two specimens according to Lunne et al. (1997), Coutinho (2007) and Coutinho (2007) modified by Andrade (2009) criteria. Based on his experience with highly plastic soft clays, Coutinho (2007) proposed a modification of Lunne et al. (1997) criterion. Andrade (2009) observed the following shortcoming in both criteria: the quality assigned to the upper bound of a class does not coincide with the quality assigned to the lower bound of the immediately above class. Andrade (2009) was able to solve this shortcoming by subdividing the classes in such a way that on the borderline of two subsequent classes, the quality to be assigned is the common term of both classes (Table 5). For instance: for $\Delta e/e_0 = 0.080$ the quality to be assigned is “fair”.

Only three specimens (CP5G, CP10D and CP10F) out of thirty two were classified below “Good to Fair” according to the Coutinho (2007) modified criterion (Table 4).

4.3 Compressibility

4.3.1 Comparison between compressibility parameters obtained from $\dot{\epsilon} = 10^{-6} \text{ s}^{-1}$ and 24-hour compression curves

Table 6 compares σ'_p , C_r and C_c values obtained from $\dot{\epsilon} = 10^{-6} \text{ s}^{-1}$ and 24-hour “ e versus σ'_v (log)” curves of series two specimens from the SFL clay layer.

The ratio between σ'_p from the $\dot{\epsilon} = 10^{-6} \text{ s}^{-1}$ compression curve, denoted by σ'_p (10^{-6} s^{-1}), and σ'_p from the 24-hour

Table 4. Quality classification of series two specimens.

Specimen	σ'_{v0} (kPa)	σ'_p (kPa)	OCR	e_0	$e(\sigma'_{v0})$	$\Delta e/e_0$	Lunne et al. (1997)	Coutinho (2007)	Coutinho (2007) modified
CP3E	53.9	100	1.9	1.49	1.39	0.067	Good to fair	Good to fair	Good to fair
CP3F	54.1	106	2.0	1.47	1.39	0.054	Good to fair	Good to fair	Very good to good
CP3G	53.7	110	2.0	1.42	1.33	0.063	Poor	Good to fair	Very good to good
CP3H	54.4	96.0	1.8	1.44	1.34	0.069	Good to fair	Good to fair	Good to fair
CP4E	60.8	125	2.1	2.25	2.17	0.036	Good to fair	Excellent to very good	Excellent to very good
CP4F	61.0	130	2.1	2.17	2.07	0.046	Good to fair	Excellent to very good	Excellent to very good
CP4G	60.6	120	2.0	2.12	2.01	0.052	Good to fair	Good to fair	Very good to good
CP4H	61.3	142	2.3	2.19	2.11	0.037	Good to fair	Excellent to very good	Excellent to very good
CP5E	65.6	137	2.1	2.26	2.14	0.053	Poor	Good to fair	Very good to good
CP5F	65.9	144	2.2	2.18	2.08	0.046	Good to fair	Excellent to very good	Excellent to very good
CP5G	65.5	101	1.5	2.25	2.05	0.089	Poor	Poor	Fair to poor
CP5H	66.1	136	2.1	2.14	2.03	0.051	Poor	Good to fair	Very good to good
CP6E	70.9	171	2.4	2.43	2.29	0.058	Poor	Good to fair	Very good to good
CP6F	71.0	169	2.4	2.40	2.29	0.046	Good to fair	Excellent to very good	Excellent to very good
CP6G	70.8	164	2.3	2.34	2.20	0.060	Poor	Good to fair	Very good to good
CP6H	71.5	167	2.3	2.41	2.32	0.037	Good to fair	Excellent to very good	Excellent to very good
CP7E	75.3	136	1.8	2.53	2.38	0.059	Good to fair	Good to fair	Very good to good
CP7F	75.5	140	1.9	2.42	2.29	0.054	Good to fair	Good to fair	Very good to good
CP7G	74.9	141	1.9	2.41	2.28	0.054	Good to fair	Good to fair	Very good to good
CP7H	75.7	138	1.8	2.49	2.35	0.056	Good to fair	Good to fair	Very good to good
CP8C	80.1	144	1.8	2.18	2.07	0.050	Good to fair	Good to fair	Very good
CP8D	80.3	138	1.7	2.19	2.07	0.055	Good to fair	Good to fair	Very good to good
CP8E	80.0	154	1.9	2.15	2.00	0.070	AMBIGUOUS	Good to fair	Good to fair
CP8F	80.4	138	1.7	2.19	2.06	0.059	Good to fair	Good to fair	Very good to good
CP9C	90.8	176	1.9	2.09	1.96	0.062	Good to fair	Good to fair	Very good to good
CP9D	91.0	182	2.0	1.98	1.87	0.056	AMBIGUOUS	Good to fair	Very good to good
CP9E	90.7	174	1.9	1.99	1.87	0.060	Good to fair	Good to fair	Very good to good
CP9F	91.1	166	1.8	1.96	1.86	0.051	Good to fair	Good to fair	Very good to good
CP10C	102	171	1.7	2.13	2.02	0.052	Good to fair	Good to fair	Very good to good
CP10D	102	162	1.6	1.98	1.82	0.081	Poor	Poor	Fair to poor
CP10E	102	179	1.8	1.97	1.84	0.066	Good to fair	Good to fair	Good to fair
CP10F	102	158	1.5	1.91	1.72	0.099	Poor	Poor	Fair to poor

Table 5. Coutinho (2007) modified by Andrade (2009) criterion for specimen quality classification.

OCR	$\Delta e/e_0$					
	Excellent to Very good	Very good to Good	Good to Fair	Fair to Poor	Poor to Very poor	Very poor
1→2.5	< 0.050	0.050 to 0.065	0.065 to 0.080	0.080 to 0.110	0.110 to 0.140	> 0.140

compression curve, denoted by σ'_p (24 h), is within 1.03 and 1.12, with an average of 1.08, which is among the rate effects described by Graham et al. (1983), Leroueil et al. (1985) and Crawford (1986). For the Santos soft clay studied herein, σ'_p (10^{-6} s^{-1}) is 8% higher, on average, than σ'_p (24 h). As shown by Leroueil et al. (1985), σ'_p depends on the strain rate adopted to plot the one-dimensional compression curve “ e versus σ'_v (log)”, σ'_p being higher, the higher the strain rate. This phenomenon is associated with the squeezing out of the viscous adsorbed water layers surrounding clay

particles (Terzaghi, 1941; Taylor 1942; Lambe & Whitman 1979, pp. 299). The higher the plasticity index, the greater the thickness of the adsorbed water layer, in the sense explained by Bjerrum (1972; 1973), magnifying secondary compression. Being so, the higher the plasticity index, the wider the spacing expected between $\dot{\epsilon} = \text{constant}$ normally consolidated one-dimensional compression lines (isotaches) in the e versus σ'_v (log) plot. Therefore, the dependence of σ'_p on the strain rate is expected to be higher, the higher the clay plasticity. This also suggests that there is a viscous

Table 6. Ratio between σ'_p and compressibility parameters from $\dot{\epsilon} = 10^{-6} \text{ s}^{-1}$ and 24-hour compression curves of series two specimens from the SFL clay layer.

Specimen	$\frac{\sigma'_p(10^{-6} \text{ s}^{-1})}{\sigma'_p(24 \text{ h})}$	$\frac{C_c(10^{-6} \text{ s}^{-1})}{C_c(24 \text{ h})}$	$\frac{C_r(10^{-6} \text{ s}^{-1})}{C_r(24 \text{ h})}$
CP4E	1.11	1.02	0.89
CP4F	1.08	1.01	1.00
CP4G	1.10	1.02	0.95
CP4H	1.07	1.04	1.20
CP5E	1.09	1.04	0.89
CP5F	1.08	1.01	0.85
CP5G	1.07	0.99	1.00
CP5H	1.07	1.01	0.82
CP6E	1.08	1.02	1.05
CP6F	1.07	1.04	1.12
CP6G	1.07	0.96	0.92
CP6H	1.09	1.05	1.14
CP7E	1.11	1.04	1.00
CP7F	1.11	1.07	1.14
CP7G	1.09	1.05	1.11
CP7H	1.07	1.08	1.29
CP8C	1.09	1.07	1.22
CP8D	1.07	1.03	1.15
CP8E	1.12	1.05	1.00
CP8F	1.07	1.07	1.26
CP9C	1.05	0.95	0.59
CP9D	1.10	1.06	1.06
CP9E	1.06	0.94	1.00
CP9F	1.05	0.98	1.11
CP10C	1.05	1.02	0.84
CP10D	1.07	1.02	0.96
CP10E	1.03	0.98	0.80
CP10F	1.10	1.04	0.76

component in σ'_v , as stated by Terzaghi (1941), Taylor (1942) and Taylor (1948, pp. 245) (see also Lima, 1993; Garcia, 1996; Santa Maria, 2002; Aguiar, 2008; Andrade, 2009). Nevertheless, a detailed discussion on this subject is out of scope of this article and will be presented in another article where the long-term loading stages run to investigate secondary consolidation and stress relaxation will be shown.

The ratio between C_c from the $\dot{\epsilon} = 10^{-6} \text{ s}^{-1}$ compression curve, denoted by $C_c(10^{-6} \text{ s}^{-1})$, and C_c from the 24-hour compression curve, denoted by $C_c(24 \text{ h})$, is within 0.94 and 1.08, with an average of 1.02. The ratio between C_r from the $\dot{\epsilon} = 10^{-6} \text{ s}^{-1}$ compression curve, denoted by $C_r(10^{-6} \text{ s}^{-1})$, and C_r from the 24-hour compression curve, denoted by $C_r(24 \text{ h})$, is within 0.76 to 1.29, with an average of 1.02 (value of 0.59 not included). A practical conclusion is that it is possible to reduce the total duration of a consolidation test from ten to about three days by using the $\dot{\epsilon} = 10^{-6} \text{ s}^{-1}$ loading criterion without changes in C_c and C_r values.

Table 7. Comparison between SFL clay compressibility parameters obtained in this study and those presented by Massad (2009).

Parameter	Massad (2009)	present study
σ'_p (kPa)	30-200	120-182
OCR	1.5-2.5	1.7-2.4
C_c/C_c	0.05-0.14 (average: 0.08)	0.06-0.14 (average: 0.11)
$C_c/(1+e_0)$	0.33-0.51 (average: 0.43)	0.46-0.68 (average: 0.56)

4.3.2 Comparison between the SFL clay layer compressibility parameters obtained in this study and by Massad (2009)

Since the Massad (2009) compressibility parameters are interpreted as having been obtained from 24-hour compression curves, only the compressibility parameters obtained in the same way are considered for comparison purposes.

Table 7 shows the ranges of SFL clay compressibility parameters presented by Massad (2009, Tables 5.1 and 5.2) and those obtained from series two specimens from samples SRA203(4) to SRA203(10), disregarding specimens CP5G, CP10D and CP10F, classified as “fair to poor” according to Coutinho (2007) modified criterion.

The σ'_p , OCR and C_c/C_c obtained in this study are within the ranges presented by Massad (2009). However, the lower and upper bounds of the $C_c/(1+e_0)$ range in this study are higher than those presented by Massad (2009), with the average in this study being higher than the upper bound of the Massad (2009) range.

The series two specimens of samples SRA203(6) and SRA203(7) showed $C_c/(1+e_0)$ within 0.60 and 0.68, whereas all the other series two specimens from samples SRA203(4) to SRA203(10) showed $C_c/(1+e_0)$ within 0.46 and 0.59 (average of 0.52). Nevertheless, even excluding samples SRA203(6) and SRA203(7), the $C_c/(1+e_0)$ values are still higher than the Massad (2009) values. Since disturbance decreases the compressibility in the virgin compression domain, Massad (2009) specimens seem to be of poorer quality than the ones studied herein, which is corroborated by the straight shape of the virgin compression lines shown by Massad (2009, Figures 5.43, 5.45 and 5.46), a disturbance effect also discussed in section 4.2.

It must be pointed out that Santos soft clay compressibility data available in the literature were mainly obtained before the nineties, when sampling standards and testing procedures were different from the current ones.

Unfortunately, in civil engineering practice, even today, sampling and testing procedures do not usually receive due care recommended by current standards. The authors' intention is to highlight the importance of following rigorously the current standards as well as special technical specifications (see Ladd & DeGroot, 2003) in order to obtain better-quality results.

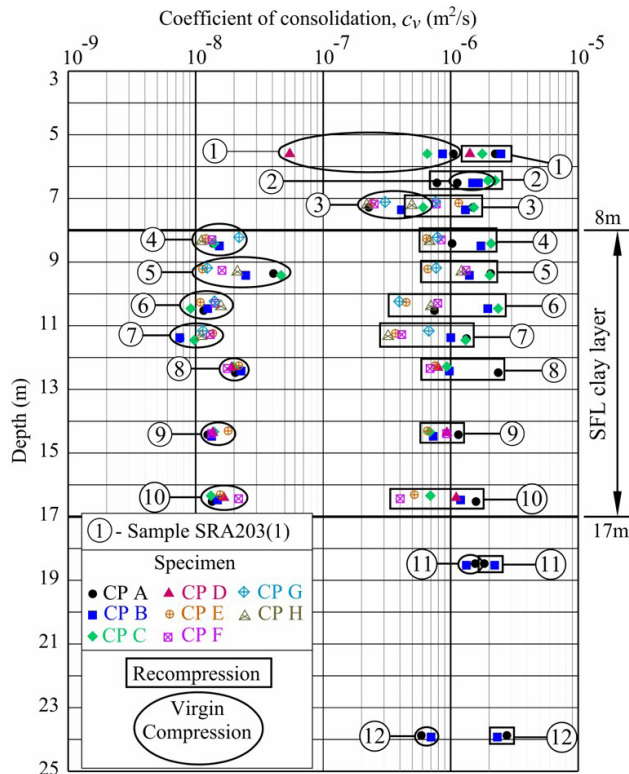


Figure 11. Coefficient of consolidation (c_v) average values profile.

4.4 Coefficient of consolidation

Figure 11 shows the c_v average values profile in the recompression (between σ'_{v0} and σ'_p) and virgin compression domain of all undisturbed specimens. Except for sample SRA203(2), which is sand, for all specimens, c_v values in the recompression domain are higher than those in the virgin compression domain. The sandy specimens, which do not belong to the SFL clay layer, showed smaller differences between c_v values from the two domains than the SFL clay specimens.

The SFL clay specimens showed c_v values in the recompression domain within $3.0 \times 10^{-7} \text{ m}^2/\text{s}$ and $2.5 \times 10^{-6} \text{ m}^2/\text{s}$. In the virgin compression domain, c_v values are within $7.0 \times 10^{-9} \text{ m}^2/\text{s}$ and $5.0 \times 10^{-8} \text{ m}^2/\text{s}$, the values between $1.0 \times 10^{-8} \text{ m}^2/\text{s}$ and $2.5 \times 10^{-8} \text{ m}^2/\text{s}$ being more frequent.

5. Conclusions

- 1) The stratigraphy of the Santos soft clay deposit near Barnabé Island follows the genetic pattern described by Massad (2009).
- 2) Following ABNT (1997) and additional cares in sampling, transportation, storage and specimen trimming (Aguiar, 2008; Andrade, 2009), high-quality one-dimensional consolidation test specimens were obtained.
- 3) Comparison between undisturbed and remolded specimen compression curves evidenced all the

remolding effects described by Ladd (1973), Coutinho (1976) and Martins (1983).

- 4) In the authors' experience with highly plastic clays, incremental loading one-dimensional consolidation tests, which usually last ten days adopting 24-hour loading stages on double drained 20 mm-high specimens, are reduced to three days by starting a new loading stage whenever $\dot{\epsilon} = 10^{-6} \text{ s}^{-1}$.
- 5) Series two tests showed 24-hour "e versus σ'_v (log)" curves displaced to the left of the $\dot{\epsilon} = 10^{-6} \text{ s}^{-1}$ "e versus σ'_v (log)" curves, keeping C_r and C_c average values unchanged.
- 6) For the Santos soft clay studied herein, σ'_p from 24-hour compression curve is about 8% lower than σ'_p from $\dot{\epsilon} = 10^{-6} \text{ s}^{-1}$ compression curve, confirming that σ'_p depends on strain rate.
- 7) SFL clay $C_c/(1+e_0)$ values of this study are higher than those presented by Massad (2009). Since disturbance decreases the compressibility in the virgin compression region, Massad (2009) specimens seem to be of poorer quality than the ones studied herein.
- 8) It is feasible to carry out a high-quality laboratory test program for design purposes following current standards rigorously.

Acknowledgements

The authors thank EMBRAPORT on behalf of engineer Juvencio Pires Terra for having taken the samples and transported them to the *Soils Rheology Laboratory* (UFRJ) and engineer Silvia Suzuki for having supervised the sampling operations. The authors are indebted to Luis Carlos de Oliveira, from COPPE/UFRJ, who diligently performed the characterization tests. The authors are also very grateful to Alexandre Oliveira da Silva, from *Mecasolo Engenharia e Consultoria Eireli*, for having prepared the figures. Finally, the authors thank to *Conselho Nacional de Desenvolvimento Científico e Tecnológico* (CNPQ) for having provided financial support for the Master's in Science researches of the two first authors.

Declaration of interest

The authors have no conflicts of interest to declare. All co-authors have observed and affirmed the contents of the paper and there is no financial interest to report.

Authors' contributions

Vitor Nascimento Aguiar: conceptualization, Data curation, Formal Analysis, Funding acquisition, Investigation, Visualization, Writing - original draft, Writing

- review & editing. Maurício do Espírito Santo Andrade: conceptualization, Data curation, Formal Analysis, Funding acquisition, Investigation, Visualization, Writing - original draft, Writing - review & editing. Ian Schumann Marques Martins: conceptualization, Investigation, Methodology, Project administration, Resources, Supervision, Visualization, Writing - review & editing. Jean Pierre Paul Rémy: conceptualization, Resources, Supervision, Validation, Writing - review & editing. Paulo Eduardo Lima de Santa Maria: conceptualization, Resources, Supervision, Validation, Writing - review & editing.

List of symbols

c_v	Coefficient of consolidation
C_c	Compression index
C_r	Recompression index
C_s	Swelling index
CP	Specimen
e	Void ratio
e_0	Natural void ratio
G_s	Specific gravity
H	Specimen height
i	Order of dial reading
I_p	Plasticity index
N	SPT blow count
OCR	Overconsolidation ratio
OM	Organic matter content
S_r	Degree of saturation
SFL	Fluvial-lagoon-bay sediments
SPM	Borehole for standard penetration tests
SPT	Standard penetration test
SRA	Borehole for taking undisturbed samples
t	Time
w	Water content
w_L	Liquid limit
W.L.	Water level
w_p	Plastic limit
ΔH	Specimen settlement
$\Delta\sigma / \sigma$	Stress ratio increment
Δt	Time elapsed between dial readings of order i and $i + 1$
ε	Specimen vertical strain
$\dot{\varepsilon}$	Specimen vertical strain rate
γ	Unit weight of soil
σ'_p	Preconsolidation (yield) stress
σ'_v	Vertical effective stress
σ'_{v0}	Effective overburden stress

References

- Aguiar, V.N. (2008). *Consolidation characteristics of the Santos harbor channel clay near Barnabé Island* [Master's dissertation, Federal University of Rio de Janeiro]. Federal University of Rio de Janeiro's repository (in Portuguese).
- American Society for Testing and Materials – ASTM. (2007). *ASTM D4220-95: standard practices for preserving and transporting soil samples*. West Conshohocken: ASTM International. <https://doi.org/10.1520/D4220.95R07>.
- Andrade, M.E.A. (2009). *Contribution to the study of soft clays from the city of Santos* [Master's dissertation, Federal University of Rio de Janeiro]. Federal University of Rio de Janeiro's repository (in Portuguese).
- Associação Brasileira de Normas Técnicas – ABNT. (1995). *ABNT NBR 6502: rocks and soils: terminology*. Rio de Janeiro: ABNT (in Portuguese).
- Associação Brasileira de Normas Técnicas – ABNT. (1997). *ABNT NBR 9820: assessment of undisturbed low consistency soil samples from boreholes*. Rio de Janeiro: ABNT (in Portuguese).
- Bjerrum, L. (1972). Embankments on soft ground: state-of-the-art Report. In *Proceedings of the ASCE Specialty Conference on Performance of Earth and Earth Supported Structures* (Vol. 2, pp. 1-54). Lafayette: Purdue University.
- Bjerrum, L. (1973). Problems of soil mechanics and construction on soft clays and structurally unstable soils (collapsible, expansive and others). In *Proceedings of the 8th International Conference on Soil Mechanics and Foundation Engineering* (Vol. 3, pp. 111-159), Moscow.
- Coutinho, R.Q. (1976). *Características de adensamento com drenagem radial de uma argila mole da Baixada Fluminense* [Master's dissertation, Federal University of Rio de Janeiro]. Federal University of Rio de Janeiro's repository (in Portuguese).
- Coutinho, R.Q. (2007). Characterization and engineering properties of Recife soft clays - Brazil. In *Proceedings of the Second International Workshop on Characterisation and Engineering Properties of Natural Soils* (Vol. 3, pp. 2049-2100). Singapore: Balkema.
- Crawford, C.B. (1986). State of the art: evaluation and interpretation of soil consolidation tests. In *Proceedings of the Symposium Sponsored by ASTM Committee D-18 on Soil and Rock* (ASTM Special Technical Publication, No. 892, pp. 71-103). West Conshohocken: ASTM.
- Garcia, S.G.F. (1996). *Relationship between secondary consolidation and stress relaxation of a soft clay in oedometric compression* [Master's dissertation, Federal University of Rio de Janeiro]. Federal University of Rio de Janeiro's repository (in Portuguese).
- Graham, J., Crooks, J.H.A., & Bell, A.L. (1983). Time effects on the stress-strain behavior of natural soft clays. *Geotechnique*, 33(3), 327-340. <http://dx.doi.org/10.1680/geot.1983.33.3.327>.
- Ladd, C.C. (1973). *Estimating settlements of structures supported on cohesive soils* (MIT 1971 Special Summer Program 1.34s). Cambridge: MIT.
- Ladd, C.C., & DeGroot, D. (2003). Recommended practice for soft ground site characterization: Arthur Casagrande Lecture. In *Proceedings of the 12th Pan-American Conference on Soil Mechanics and Geotechnical Engineering* (Vol. 1, 3-57), Boston.
- Lambe, T.W., & Whitman, R.V. (1979). *Soil mechanics* (SI version). New York: John Wiley & Sons.

- Leroueil, S., Kabbaj, M., Tavenas, F., & Bouchard, R. (1985). Stress-strain-strain rate relation for the compressibility of sensitive natural clays. *Geotechnique*, 35(2), 159-180. <http://dx.doi.org/10.1680/geot.1985.35.2.159>.
- Lima, G.P. (1993). *A non-linear theory of consolidation* [Master's dissertation, Federal University of Rio de Janeiro]. Federal University of Rio de Janeiro's repository (in Portuguese).
- Lunne, T., Berre, T., & Strandvik, S. (1997). Sample disturbance effects in soft low plastic Norwegian clay. In *Proceedings of the Symposium on Recent Developments in Soil and Pavement Mechanics* (pp. 81-102), Rio de Janeiro.
- Martins, I.S.M. (1983). *Sobre uma nova relação índice de vazios tensão em solos* [Master's dissertation, Federal University of Rio de Janeiro]. Federal University of Rio de Janeiro's repository (in Portuguese).
- Massad, F. (1985). *Argilas quaternárias da Baixada Santista: características e propriedades geotécnicas* [Habilitation thesis, University of São Paulo]. University of São Paulo's repository (in Portuguese).
- Massad, F. (2009). *Solos marinhos da Baixada Santista: características e propriedades geotécnicas*. São Paulo: Oficina de Textos (in Portuguese).
- Rémy, J.P.P., Martins, I.S.M., Santa Maria, P.E.L., Aguiar, V.N., & Andrade, M.E.S. (2011). Working hypothesis, special laboratory tests, working tools, analysis of the monitoring of a pilot embankment built on soft clay in Santos with wick drains and its application to the final design. *Soil and Rocks*, 34(4), 277-316.
- Santa Maria, F.C.M. (2002). *Rheological experimental study of the coefficient of earth pressure at rest, K₀* [Doctoral thesis, Federal University of Rio de Janeiro]. Federal University of Rio de Janeiro's repository (in Portuguese).
- Silva, F.P. (1970). Uma nova construção gráfica para determinação da pressão de pré-adensamento de uma amostra de solo. In *Anais do 4º Congresso Brasileiro de Mecânica dos Solos e Engenharia de Fundações* (Vol. 2, No. 1, pp. 219-223). Rio de Janeiro: ABMS.
- Suguio, K., & Martin, L. (1994). Geologia do quaternário. In F.F. Falconi & A. Nigro Junior (Eds.), *Solos do litoral de São Paulo* (pp. 235-264). São Paulo: ABMS-NRSP.
- Taylor, D.W. (1942). *Research on consolidation of clays* (Serial, No. 82). Massachusetts: Department of Civil and Sanitary Engineering, Massachusetts Institute of Technology.
- Taylor, D.W. (1948). *Fundamentals of soil mechanics*. London: John Wiley & Sons.
- Terzaghi, K. (1941). Undisturbed clay samples and undisturbed clays. *Journal of the Boston Society of Civil Engineers*, 28(3), 45-65.

Appendix A. σ'_p and compressibility parameters.

Table A1. σ'_p and compressibility parameters of all specimens (series one and two) obtained from e versus σ'_v (log) curves corresponding to $\dot{\epsilon} = 10^{-6} \text{ s}^{-1}$.

Specimen	Depth (m)	Test series	e_0	σ'_p (kPa)	C_c	$C_c/(1+e_0)$	C_r	C_r/C_c
CP1A	5.55 - 5.65	1	1.30	100	0.48	0.21	0.08	0.17
CP1B	5.55 - 5.65	1	1.35	100	0.46	0.20	0.09	0.20
CP1C	5.55 - 5.65	1	1.37	92	0.51	0.22	0.09	0.18
CP1D	5.55 - 5.65	1	1.44	90	0.57	0.23	0.10	0.18
CP2A	6.48 - 6.55	1	1.07	42	0.26	0.13	^(b)	^(b)
CP2B	6.48 - 6.55	1	1.11	48	0.27	0.13	^(b)	^(b)
CP2C	6.40 - 6.48	1	1.00	58	0.24	0.12	^(b)	^(b)
CP2D ^(a)	6.40 - 6.48	1	1.11	23	0.22	0.10	^(b)	^(b)
CP3A	7.25 - 7.32	1	1.55	105	0.80	0.31	0.10	0.13
CP3B	7.32 - 7.40	1	1.69	100	0.86	0.32	0.10	0.12
CP3C	7.25 - 7.32	1	1.52	120	0.66	0.26	0.11	0.17
CP3D ^(a)	7.32 - 7.40	1	1.83	35	0.67	0.23	^(b)	^(b)
CP3E	7.13 - 7.16	2	1.49	110	0.78	0.31	0.12	0.15
CP3F	7.16 - 7.19	2	1.47	119	0.72	0.29	0.15	0.21
CP3G	7.10 - 7.13	2	1.42	120	0.77	0.32	0.11	0.14
CP3H	7.19 - 7.25	2	1.44	105	0.69	0.28	0.16	0.23
CP4A	8.38 - 8.46	1	2.24	170	1.91	0.59	0.14	0.07
CP4B	8.46 - 8.53	1	2.26	165	1.73	0.53	0.19	0.11
CP4C	8.38 - 8.46	1	2.17	170	1.89	0.60	0.19	0.10
CP4D ^(a)	8.46 - 8.53	1	2.31	70	0.90	0.27	0.47	0.52
CP4E	8.24 - 8.28	2	2.25	139	1.72	0.53	0.16	0.09
CP4F	8.28 - 8.32	2	2.17	140	1.69	0.53	0.16	0.09
CP4G	8.20 - 8.24	2	2.12	132	1.69	0.54	0.19	0.11
CP4H	8.32 - 8.38	2	2.19	152	1.86	0.58	0.12	0.06
CP5A	9.34 - 9.39	1	1.97	170	1.56	0.53	0.17	0.11
CP5B	9.39 - 9.45	1	2.02	165	1.53	0.51	0.20	0.13
CP5C	9.39 - 9.45	1	2.14	155	1.42	0.45	0.18	0.13
CP5D ^(a)	9.45 - 9.53	1	2.13	65	0.66	0.21	0.50	0.76
CP5E	9.20 - 9.24	2	2.26	149	1.64	0.50	0.17	0.10
CP5F	9.24 - 9.28	2	2.18	156	1.56	0.49	0.17	0.11
CP5G	9.17 - 9.20	2	2.25	108	1.28	0.39	0.41	0.32
CP5H	9.28 - 9.34	2	2.14	145	1.44	0.46	0.14	0.10
CP6A	10.50 - 10.55	1	2.53	175	2.22	0.63	0.15	0.07
CP6B	10.43 - 10.50	1	2.57	175	2.18	0.61	0.20	0.09
CP6C	10.43 - 10.50	1	2.60	180	2.37	0.66	0.21	0.09
CP6D ^(a)	10.43 - 10.50	1	2.58	80	1.17	0.33	^(b)	^(b)
CP6E	10.25 - 10.28	2	2.43	185	2.23	0.65	0.21	0.09
CP6F	10.28 - 10.31	2	2.40	181	2.35	0.69	0.19	0.08
CP6G	10.22 - 10.25	2	2.34	176	1.93	0.58	0.22	0.11
CP6H	10.36 - 10.41	2	2.41	182	2.44	0.72	0.16	0.07
CP7A	11.39 - 11.42	1	2.35	160	2.06	0.61	0.23	0.11
CP7B	11.36 - 11.39	1	2.43	150	1.96	0.57	0.30	0.15
CP7C	11.42 - 11.49	1	2.21	155	1.73	0.54	0.27	0.16
CP7D ^(a)	11.42 - 11.49	1	2.18	55	0.95	0.30	0.45	0.47
CP7E	11.22 - 11.26	2	2.53	151	2.29	0.65	0.22	0.10
CP7F	11.26 - 11.30	2	2.42	155	2.24	0.65	0.25	0.11
CP7G	11.14 - 11.18	2	2.41	153	2.27	0.67	0.21	0.09
CP7H	11.30 - 11.36	2	2.49	148	2.39	0.68	0.22	0.09

^(a)specimen remolded in the laboratory; ^(b)see discussion in section 4.2.

Table A1. Continued...

Specimen	Depth (m)	Test series	e_0	σ'_p (kPa)	C_c	$C_c/(1+e_0)$	C_r	C_r/C_c
CP8A	12.45 - 12.50	1	2.22	145	1.67	0.52	0.22	0.13
CP8B	12.40 - 12.45	1	2.14	130	1.54	0.49	0.24	0.16
CP8C	12.27 - 12.30	2	2.18	157	1.76	0.55	0.22	0.13
CP8D	12.30 - 12.33	2	2.19	147	1.76	0.55	0.23	0.13
CP8E	12.24 - 12.27	2	2.15	173	1.82	0.58	0.18	0.10
CP8F	12.33 - 12.36	2	2.19	148	1.85	0.58	0.24	0.13
CP9A	14.40 - 14.45	1	1.90	200	1.41	0.49	0.24	0.17
CP9B	14.45 - 14.50	1	1.93	200	1.46	0.50	0.16	0.11
CP9C	14.32 - 14.35	2	2.09	184	1.46	0.47	0.13	0.09
CP9D	14.35 - 14.38	2	1.98	200	1.50	0.50	0.18	0.12
CP9E	14.29 - 14.32	2	1.99	184	1.63	0.55	0.15	0.09
CP9F	14.38 - 14.40	2	1.96	174	1.41	0.48	0.20	0.14
CP10A	16.50 - 16.55	1	1.87	200	1.80	0.63	0.17	0.09
CP10B	16.45 - 16.50	1	1.93	190	1.86	0.63	0.33	0.18
CP10C	16.33 - 16.36	2	2.13	179	1.87	0.60	0.21	0.11
CP10D	16.39 - 16.42	2	1.98	174	1.61	0.54	0.26	0.16
CP10E	16.29 - 16.33	2	1.97	184	1.60	0.54	0.16	0.10
CP10F	16.42 - 16.45	2	1.91	174	1.70	0.58	0.16	0.09
CP11A	18.45 - 18.50	1	0.98	150	0.30	0.15	0.09	0.30
CP11B	18.50 - 18.55	1	0.96	160	0.31	0.16	0.07	0.23
CP12A	23.85 - 23.90	1	0.73	94	0.08	0.05	^(b)	^(b)
CP12B	23.90 - 23.95	1	0.70	94	0.11	0.06	^(b)	^(b)

^(a)specimen remolded in the laboratory; ^(b)see discussion in section 4.2.

Table A2. σ'_p and compressibility parameters of series two specimens obtained from e versus σ'_v (log) curves corresponding to 24 hours.

Specimen	Depth (m)	e_0	σ'_p (kPa)	C_c	$C_c/(1+e_0)$	C_r	C_r/C_c	C_s
CP3E	7.13 - 7.16	1.49	100	0.74	0.30	0.17	0.23	0.05
CP3F	7.16 - 7.19	1.47	106	0.71	0.29	0.18	0.25	0.05
CP3G	7.10 - 7.13	1.42	110	0.81	0.33	0.14	0.17	0.05
CP3H	7.19 - 7.25	1.44	96	0.70	0.29	0.19	0.27	0.05
CP4E	8.24 - 8.28	2.25	125	1.69	0.52	0.18	0.11	0.13
CP4F	8.28 - 8.32	2.17	130	1.68	0.53	0.16	0.10	0.13
CP4G	8.20 - 8.24	2.12	120	1.66	0.53	0.20	0.12	0.12
CP4H	8.32 - 8.38	2.19	142	1.78	0.56	0.10	0.06	0.14
CP5E	9.20 - 9.24	2.26	137	1.57	0.48	0.19	0.12	0.13
CP5F	9.24 - 9.28	2.18	144	1.55	0.49	0.20	0.13	0.13
CP5G	9.17 - 9.20	2.25	101	1.29	0.40	0.41	0.32	0.14
CP5H	9.28 - 9.34	2.14	136	1.43	0.46	0.17	0.12	0.11
CP6E	10.25 - 10.28	2.43	171	2.18	0.64	0.20	0.09	0.18
CP6F	10.28 - 10.31	2.40	169	2.27	0.67	0.17	0.07	0.18
CP6G	10.22 - 10.25	2.34	164	2.02	0.60	0.24	0.12	0.18
CP6H	10.36 - 10.41	2.41	167	2.33	0.68	0.14	0.06	0.16
CP7E	11.22 - 11.26	2.53	136	2.20	0.62	0.22	0.10	0.15
CP7F	11.26 - 11.30	2.42	140	2.10	0.61	0.22	0.10	0.15
CP7G	11.14 - 11.18	2.41	141	2.17	0.64	0.19	0.09	0.16
CP7H	11.30 - 11.36	2.49	138	2.21	0.63	0.17	0.08	0.16
CP8C	12.27 - 12.30	2.18	144	1.64	0.52	0.18	0.11	0.10
CP8D	12.30 - 12.33	2.19	138	1.71	0.54	0.20	0.12	0.10
CP8E	12.24 - 12.27	2.15	154	1.73	0.55	0.18	0.10	0.11
CP8F	12.33 - 12.36	2.19	138	1.73	0.54	0.19	0.11	0.10
CP9C	14.32 - 14.35	2.09	176	1.54	0.50	0.22	0.14	0.13

Table A2. Continued...

Specimen	Depth (m)	e_0	σ'_p (kPa)	C_c	$C_c/(1+e_0)$	C_r	C_r/C_c	C_s
CP9D	14.35 - 14.38	1.98	182	1.41	0.47	0.17	0.12	0.13
CP9E	14.29 - 14.32	1.99	174	1.73	0.58	0.15	0.09	0.13
CP9F	14.38 - 14.40	1.96	166	1.44	0.49	0.18	0.13	0.12
CP10C	16.33 - 16.36	2.13	171	1.84	0.59	0.25	0.14	0.15
CP10D	16.39 - 16.42	1.98	162	1.58	0.53	0.27	0.17	0.12
CP10E	16.29 - 16.33	1.97	179	1.63	0.55	0.20	0.12	0.13
CP10F	16.42 - 16.45	1.91	158	1.63	0.56	0.21	0.13	0.11